Arabian Journal of Chemistry (2017) **10**, S627–S635

King Saud University

Arabian Journal of Chemistry

www.ksu.edu.sa
www.sciencedirect.com

ORIGINAL ARTICLE

The water soluble composite poly-(vinylpyrrolidone–methylaniline): A new class of corrosion inhibitors of mild steel in hydrochloric acid media

R. Karthikaiselvi [a,*], **S. Subhashini** [b]

[a] *Department of Chemistry, Kumaraguru College of Technology, Coimbatore, Tamil Nadu, India*
[b] *Department of Chemistry, Avinashilingam University for Women, Coimbatore, Tamil Nadu, India*

Received 7 June 2012; accepted 27 October 2012
Available online 16 November 2012

KEYWORDS

Adsorption;
Corrosion inhibitor;
Impedance;
Scanning electron microscope;
FTIR;
EDX

Abstract In recent years poly methyl aniline has been reported as one of the efficient corrosion inhibitors of mild steel in acidic media. In view of the major limitation of the insolubility of poly-methyl aniline PMA, we propose to convert PMA into a water soluble composite using supporting polymer polyvinylpyrrolidone to get higher solubility and corrosion inhibition efficiency. The water soluble composite poly(vinylpyrrolidone-methyl aniline) was synthesized by chemical oxidative polymerization and its inhibitive effect on mild steel in 1 M HCl has been investigated using weight loss and electrochemical techniques (potentiodynamic polarization studies and impedance spectroscopy). SEM and EDX analyses are carried out to establish a protective film formation on the metal surface.

1. Introduction

Acid solutions are commonly used for the removal of undesirable scale and rust in metal working, in the chemical cleaning of scales in metallurgy and in the petrochemical industry (Obi-Egbedi and Obot, 2012).To prevent unwanted metal dissolution and excess acid consumption in the pickling process of mild steel, inhibitors are added to the acid (Ahamad and Quraishi, 2009). Efficient corrosion inhibitors used to prevent the deterioration of mild steel are heterocyclic organic compounds consisting of a π-system and/or O, N, S heteroatoms. (El-Taib Heakala et al., 2011; Kokalj, 2010; Obot et al., 2010; Obot and Obi-Egbedi, 2010; Ebenso et al., 2008; Umoren and Ebenso, 2007; Lebrini et al., 2006). The initial mechanism in any corrosion inhibition process is the adsorption of the inhibitor on the metal surface. The effectiveness of the adsorption depends on the nature and surface charge of the metal, the corroding medium and the chemical structure of the inhibitor molecules such as functional groups, aromaticity,

* Corresponding author. Tel.: +91 9543966652; fax: +91 422 2669406.
E-mail address: karthidilip27@gmail.com (R. Karthikaiselvi).

Peer review under responsibility of the King Saud University.

ELSEVIER Production and hosting by Elsevier

http://dx.doi.org/10.1016/j.arabjc.2012.10.024
1878-5352

p-orbital character of the donating electron, steric factor, and electron density of the donor atoms (El-Naggar, 2007).

Polymers are also used as corrosion inhibitors because through their functional groups they form complexes with metal ions and on the metal surface these complexes occupy a large surface area thereby blanketing the surface and protecting the metal from corrosive agents present in the solution (Rajendran et al., 2005). The inhibitive power of these polymers is related structurally to the cyclic rings and hetero atoms (oxygen and nitrogen) which are the major reactive centers of adsorption. Poly (*o*-toluidine) coating has been electrosynthesized on copper to prevent the corrosion. (Shinde et al., 2005).Corrosion inhibition of mild steel by polyethylene glycol and polyvinyl alcohol has also been reported (Umoren et al., 2006). Copolymer poly (*o*-aniline-*co*-*o*-toluidine) coating has been electrosynthesized on mild steel (Borole et al., 2006). Poly (*o*-anisidine-*co*-*o*-toluidine), as a strong adherent coating on Cu substrates, was electrosynthesised using cyclic voltammetry (Pritee et al., 2007).

Since PMA is a good corrosion inhibitor of iron, many studies have been reported on the corrosion protection of mild steel in acid. The great potentiality of PMA still remains completely unexploited because of its instability and insolubility in common organic solvents and water. To circumvent this problem a new approach has been taken to prepare water soluble composites and blends using supporting polymers such as polyvinyl pyrrolidone hence are used as effective inhibitors. It is nontoxic. It acts as a steric stabilizer and prevents the precipitation of polymerized methyl aniline and makes it finely dispersed in solution. The synthesized composite was tested as a corrosion inhibitor on mild steel in hydrochloric acid medium.

In the present work the water soluble composite poly (vinyl pyrrolidone-methyl aniline) PVPMA is synthesized and investigated as an inhibitor for the corrosion of mild steel in 1 M HCl using weight loss, potentiodynamic polarization, electrochemical impedance spectroscopy (EIS), scanning electron microscope and energy dispersive X-ray spectroscopy.

2. Experimental details

2.1. Inhibitor synthesis

A 20 ml of PVP (10% w/w) was well mixed with 20 ml of *o*-methyl aniline in oxalic acid (1 ml in 100 ml) using a magnetic stirrer. The system was then cooled below −5 °C and followed by the addition of 20 ml of aqueous acidic (oxalic acid) solution of ammoniumpersulphate (APS). APS mole ratio was maintained as 1:1. Polymerization was allowed to proceed for 3 h and the composite was formed as a bright green stable solution (Gangopadhyay and Amitabha De Ghosh, 2001). The proposed structure of PVPMA is shown in Fig. 1.

The structural characteristics of PVPMA (Fig. 2) was investigated by FTIR spectroscopy in the range of 2000–400 cm^{-1}. Appearance of bands at 2975 and 2852 cm^{-1} are due to the presence of CH and CH_2 stretching vibrations in PVPMA (Roeges, 1994). A sharp band at 1641 cm^{-1} is due to C═O stretching of PVP (Molyneux, 1983) is shifted to 1642 cm^{-1} and subdued as a result of structural modifications primarily due to intermolecular H-bonding utilizing N-hydrogens of methyl aniline and C═O group of PVP (Ghosh et al., 1998). The band at 1418 cm^{-1} represents the stretching vibrations of the benzenoid rings. The band at 1584 cm^{-1} is indicative of stretching vibrations in the quinonoid ring (Neoh et al., 1991). The appearance of a band at 3185 cm^{-1} corresponds to the presence of an OH group in hydrophilic polyvinyl pyrrolidone. The peak at 1294 cm^{-1} is due to the amide C–N stretch of PVP (Roeges, 1994). Aromatic out-of-plane bending stands for the group of peaks appear between 900 and 630 cm^{-1} (Coates, 2000).

2.2. Specimens

Mild steel of composition (wt%) 0.084% carbon, 0.197% manganese, 0.022% silicon, 0.023% phosphorous, 0.022% sulfur, 0.028% chromium, 0.12% molybdenum, 0.015% nickel and the remaining iron was used for gravimetric and electrochemical measurements. Specimens were mechanically cut into 5×1 cm for weight loss experiments and were lacquered so as to expose an area of 1 cm^2 for all electrochemical studies. Before use, the specimens were mechanically polished with fine grade emery paper, degreased and dried in acetone and stored in a dessicator.

2.3. Reagents used

Ammonium persulphate, oxalic acid, *o*-methyl aniline and polyvinyl alcohol (M_w = 12,000) were purchased from Merck chemicals. *o*-methyl aniline was distilled prior to use. All other chemicals were used without further purification.

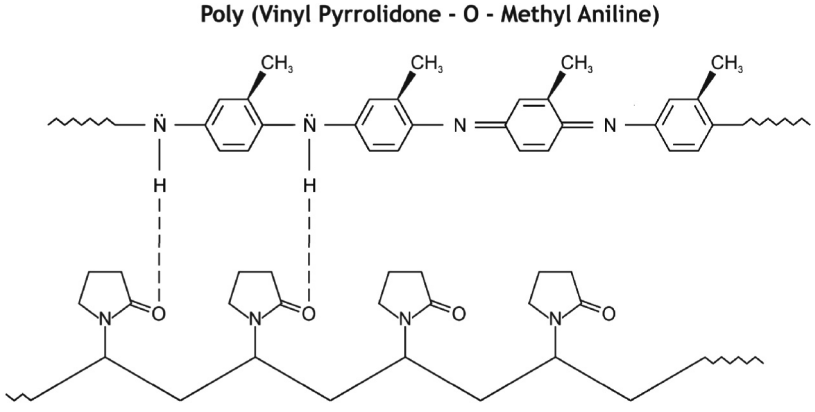

Figure 1 The proposed structure of PVPMA.

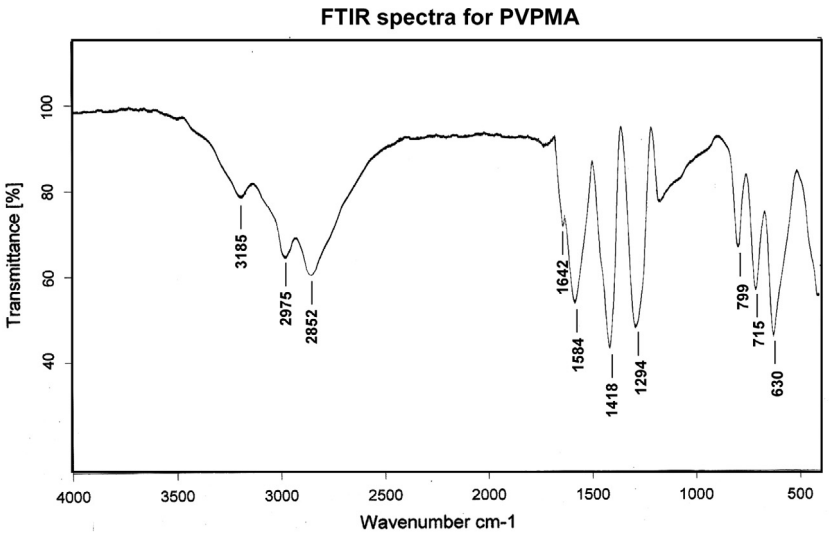

Figure 2 FTIR spectra for PVPMA.

2.4. Gravimetric measurements

The gravimetric method (weight loss) is probably the most widely used method of inhibition assessment. The simplicity and reliability of the measurement offered by the weight loss method are such that the technique forms the baseline method of measurement in many corrosion monitoring programmes. (Afidah and Kassim, 2008). Gravimetric measurements were carried out in a glass vessel containing 100 ml of 1 M HCl with and without the addition of different concentrations of PVPMA in the temperature range of 303–343 K for ½ h immersion time. All the above tests were conducted in the varying temperature with ½ h immersion time. Since, the inhibitor PVPMA is used in the boiler scale removal, more than ½ h immersion period is not required. The specimens were withdrawn, rinsed with double distilled water, washed with acetone, dried and weighed. The experiments were done in triplicate and the average value of the weight loss was noted. From the weight loss values obtained through the above experiments the corrosion rate CR was calculated using the expression

$$\mathrm{CR(mpy)} = 534W/DAT \tag{1}$$

where, W is the weight loss in g, D is the density of mild steel in g/cm^2, A is the area of the specimen in cm^2, and T is the exposure time in hours.

2.5. Electrochemical measurements

Electrochemical experiments were performed in a conventional three-electrode cell assembly with a mild steel specimen as the working electrode, a platinum foil with larger surface area as the counter electrode and saturated calomel electrode as the reference electrode.

2.5.1. Potentiodynamic polarization studies

Potentiodynamic polarization involves the characterization of a sample by its current-potential relationship. When a metal sample is in contact with an aqueous corrosive medium, both oxidation and reduction occur on its surface. For potentiodynamic polarization studies, the experiments were carried out over a potential range of −0.1 to −1.0 V with respect to the reference electrode and its current response was measured at a scan rate of 2 mV s^{-1}. Applied potential versus current was plotted and theextrapolation of the linear portion to the corrosion potential (E_{corr}) gave corrosion current (I_{corr}). In anodic and cathodic plots, the slope of the linear portion gave Tafel constants. The inhibition efficiency of the inhibitor was calculated from the I_{corr} values using the following equation

$$\mathrm{IE} = \frac{I_{corr(blank)} - I_{corr(inhibitor)}}{I_{corr(blank)}} \times 100 \tag{2}$$

where, $I_{corr(blank)}$ is corrosion current without inhibitor and $I_{corr(inhibitor)}$ is corrosion current with inhibitor.

2.5.2. Electrochemical impedance spectroscopy

A sine wave with 10 mV amplitude was used to perturb the system (Bentiss et al., 2009) and the frequency was varied from 20 kHz to 0.1 Hz. The real (z) and imaginary (z') parts of the impedance were plotted in a Nyquist diagram. The charge transfer resistance values were obtained from the plots of z versus z'. The values of (R_t + R_s) correspond to the point where the plot cuts the z axis at 10 Hz frequency and R_s corresponds to the point where the semicircle cuts the Z axis at high frequency. The difference between (R_t + R_s) and R_s provides the charge transfer resistance (R_{ct}) values. Solartron Electrochemical Analyzer Model 1280B interfaced with an IBM computer and Z plot and CorrWare softwares were used for data acquisition and analysis.

2.6. Surface analysis

The surface morphology of mild steel specimens was examined before and after exposure to 1 M HCl for 12 h with and without an inhibitor using Jeol JSM 6390 scanning electron microscope. The energy of the acceleration beam employed was 20 keV. Surface analysis of mild steel in 1 M HCl in the absence and the presence of PVPMA was performed with a INCA penta FETX3 Energy-dispersive X-ray spectrometer.

Table 1 Corrosion rate of mild steel and inhibition efficiency of PVPMA for mild steel corrosion at various temperatures.

Conc. (ppm)	303 K		313 K		323 K		333 K		343 K	
	CR (mpy)	IE (%)	CR (mpy)	IE (%)	CR (mpy)	IE (%)	CR (mpy)	IE (%)	CR (mpy)	IE (%)
Blank	1250.72		4246.69		6954.84		10823.88		15675	
100	857.37	31.45	1476.15	65.24	2279.10	67.23	5837.32	46.07	8566.39	45.35
200	817.22	34.66	1320.72	68.9	1951.53	71.94	4580.67	57.68	8381.42	46.53
400	732.67	41.42	1197.56	71.80	1822.86	73.79	3020.95	72.09	7934.69	49.38
600	675.89	45.96	1113.06	73.79	1790.18	74.26	2334.71	78.43	6003.52	61.70
800	613.10	50.98	1039.17	75.53	1677.51	75.88	1857.38	82.84	5873.42	62.53
1000	531.18	57.53	852.32	79.93	1117.64	83.93	1679.87	84.48	4809.09	69.32
2000	504.16	59.69	825.56	80.56	1107.21	84.08	1406.02	87.01	3370.13	78.50

3. Results and discussion

3.1. Gravimetric analysis

3.1.1. Effect of inhibitor concentration

The values of percentage corrosion rate (CR) and inhibition efficiency (% IE) are obtained from weight loss method at different concentrations of the inhibitor in the temperature range of 303–343 K and are summarized in Table 1. It has been found that PVPMA inhibits the corrosion of mild steel in hydrochloric acid solution at all concentrations used in this study (100–2000 ppm). Inhibition efficiency increases with increase in inhibitor concentration.

Inhibition efficiency was calculated using the formula

$$\mathrm{IE}(\%) = \frac{\mathrm{CR}_{\mathrm{Blank}} - \mathrm{CR}_{\mathrm{inhibitor}}}{\mathrm{CR}_{\mathrm{Blank}}} \times 100$$

where,

$\mathrm{CR}_{\mathrm{Blank}}$ is the Corrosion rate without inhibitor
$\mathrm{CR}_{\mathrm{inhibitor}}$ is the Corrosion rate with inhibitor

Maximum inhibition efficiency (87.01%) is shown at the 2000 ppm concentration of the inhibitor in 1 M HCl at 333 K. It is also evident from Table 1 that the corrosion rate is decreased from 1250.72 to 857.37 mpy with the addition of 100 ppm of PVPMA at 303 K.

3.1.2. Effect of temperature

The influence of solution temperature on the corrosion rate in the presence and the absence of inhibitor is shown in Fig. 3.

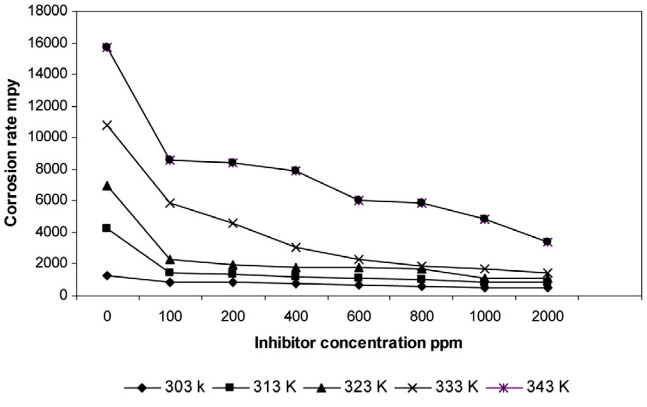

Figure 3 Effect of PVPMA concentrations on the corrosion rate of mild steel in 1 M HCl at different temperatures.

Inhibition efficiency increases with temperature up to 333 K and beyond that decrease in efficiency is observed especially in the lower concentration of PVPMA. The enhancement in inhibition efficiency at high temperatures may be due to (i) higher activation energy available for adsorption at higher temperatures (ii) enhancement in the surface coverage at high temperature by the inhibitor molecule (Chaturvedi and Chaudhary, 1990). Decrease in the inhibition efficiency at a higher temperature is due to increased rate of the dissolution process of mild steel and partial desorption of the inhibitor from the metal surface (Singh and Quraishi, 2009).

3.1.3. Thermodynamic activation parameters

Temperature is an important parameter in studies of metal dissolution. The effect of temperature on the inhibited acid metal reaction is very complex because many changes may occur on the metal surface such as rapid etching, desorption of inhibitor and that the inhibitor may undergo decomposition. The dependence of corrosion rate on temperature can be expressed by the Arrhenius equation (Quraishi and Khan, 2005)

$$\mathrm{Log\ CR} = \mathrm{Log}\ \lambda - (E_a/2.303RT) \quad (3)$$

where, CR is the corrosion rate at the absolute temperature T, E_a is the apparent activation energy, R is the molar gas constant, and λ is the frequency factor.

A plot of log of CR obtained from gravimetric measurements versus $1/T$ gave a straight line with a regression coefficient close to unity. The values of apparent activation energy E_a obtained from the slope $-E_a/2.303R$ of the lines and the pre exponential factor λ obtained from the intercept log λ are given in Table 2.

The data show that the thermodynamic activation energy (E_a) of the corrosion in mild steel in 1 M HCl solution in the presence of PVPMA is lesser than that in the free acid solution.

Table 2 Activation parameters of mild steel in 1 M HCl in the absence and the presence of PVPMA.

Conc. (ppm)	E_a (kJ mol^{-1})	λ (mg cm^{-2})	ΔH (kJ mol^{-1})	$-\Delta S$ (kJ mol^{-1} K^{-1})
Blank	52	1.89×10^9	49.55	1098.93
100	51	6.98×10^8	48.89	1099.36
200	50	4.58×10^8	48.07	1099.54
400	48	1.95×10^8	46.19	1099.92
600	44	2.70×10^7	41.26	1100.77
800	43	2.34×10^7	41.14	1100.84
1000	43	1.73×10^7	40.89	1100.97
2000	37	1.43×10^6	34.55	1102.05

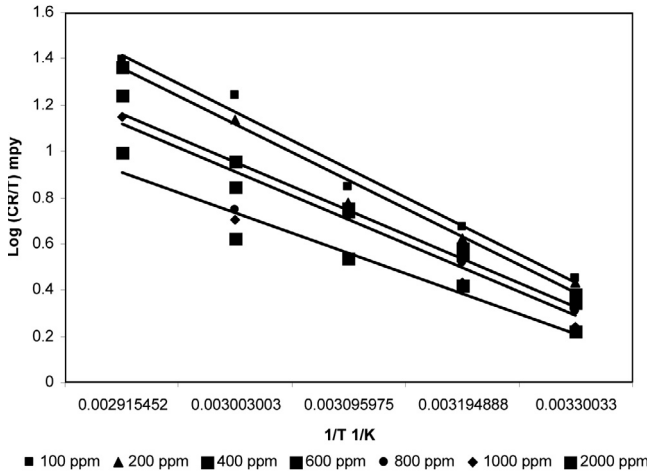

Figure 4 Transition state plot for mild steel corrosion in 1 M HCl in absence and presence of various concentrations of PVPMA.

This finding indicates that PVPMA retards the corrosion of mild steel in the examined media (Nalini et al., 2011).The value of λ is lower for the inhibited solution than for the uninhibited solution. Generally lower λ value leads to the lower corrosion rate.

The transition state equation is (Shukla et al., 2008)

$$CR = RT/Nh \exp(\Delta S/R) \exp(-\Delta H/RT) \quad (4)$$

where, h is Plank's constant, N is Avogadro's number, ΔS the entropy of activation and ΔH the enthalpy of activation. A plot of log CR/T versus $1/T$ gave a straight line (Fig. 4) with a slope of $\Delta H/2.303R$ and an intercept of log $R/Nh + \Delta S/2.303R$, from which the values of ΔS and ΔH were calculated and listed in Table 2. The positive sign of enthalpies reflects the endothermic nature of the steel dissolution process meaning that the dissolution of steel is difficult (Guan et al., 2004).The negative values of the entropy of activation both in the absence and the presence of the inhibitor imply that the activated complex in the rate determining step represents an association rather than a dissociation step, meaning that a decrease in disordering takes place ongoing from reactants to the activated complex (Tao et al., 2009; Oguzie et al., 2008).

3.1.4. Adsorption isotherm

The data were tested graphically by fitting into various adsorption isotherms including Freundlich, Temkin, and Langmuir and formulated the thermodynamic/kinetic model of El-Awady isotherms. According to this isotherm, θ is related to the inhibitor concentration by the following Eq. (5) (Morad and Kamal El-Dean, 2006).

$$Log(C/\theta) = \log C - \log K \quad (5)$$

The values of regression coefficients (R^2) confirm the validity of this approach.

Though the linearity of the plot may be taken to suggest that the adsorption of the inhibitor follows the Langmuir isotherm, the considerable deviation of the slope from unity indicates that the Langmuir adsorption isotherm could not be strictly applied. It has been postulated in the derivation of the Langmuir isotherm equation that adsorbed molecules do not interact with one another, but this is not true in the case of large molecules having polar atoms or groups which are adsorbed on the metal surface. Such adsorbed species interact by mutual repulsion or attraction that would affect the slope (Singh and Chaudhary, 1996). The deviation of the slope values (Table 3) could also be interpreted due to the changes in adsorption heat with increasing surface coverage which has been ignored in the derivation of the Langmuir isotherm (Oguzie et al., 2004).

Table 3 Adsorption parameters calculated from El-Awady adsorption isotherm.

Temperature (K)	K_{ads} (mol^{-1})	$1/y$	R^2	Slope	ΔG_{ads} (kJ mol^{-1})
303	13.543	2.312957	0.9541	0.43234	−16.69
313	848.692	3.579188	0.9406	0.27939	−28.01
323	799.097	3.139304	0.8145	0.31854	−28.74
333	85.705	1.344796	0.9739	0.74360	−23.45
343	43.316	1.961773	0.8825	0.50974	−22.20

The experimental data have been then fitted into the modified form of the Langmuir isotherm known as El-Awady kinetic–thermodynamic adsorption model which may appropriately represent the adsorption behavior of the inhibitor on the iron surface.

El –Awady isotherm is given as

$$\text{Log}(\theta/1-\theta) = \log K + y \log C \quad (6)$$

where, C is the concentration of inhibitor, θ is the surface coverage, K is the equilibrium constant for the adsorption process; $K_{ads} = K^{1/y}$, where y represents the number of inhibitor molecules occupying a given site. Value of $1/y$ less than unity implies the formation of a multi layer of the inhibitor on the metal surface, while the value of $1/y$ greater than unity means that a given inhibitor occupies more than one active site (Ibot et al., 2009). Curve fitting of the data into El-Awady thermodynamic/kinetic model is shown in Fig. 5.

It is evident from Table 3 that the value of $1/y$ is greater than unity showing that PVPMA occupies more than one active site. K_{ads} value (Table 3) decreases in the presence of PVPMA with an increase in the temperature indicating that the adsorption of PVPMA on the mild steel surface is unfavorable at higher temperatures (Lagrenee et al., 2002). Large val-

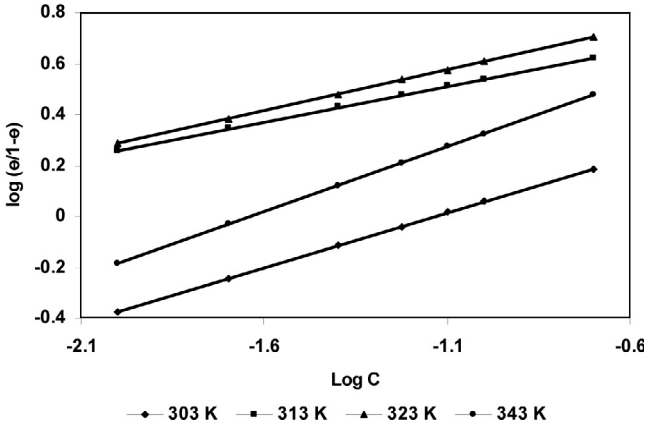

Figure 5 El-Awady adsorption isotherm model for mild steel in 1 M HCl containing PVPMA at different temperatures.

ues of K_{ads} mean better inhibition efficiency of a given inhibitor and a strong electric interaction between the double layer existing at the phase boundary and the adsorbed species. Small values of K_{ads} however, compromise that such interactions are weaker, denoting that the adsorbed species are easily replaceable by the solvent molecules from the surface (Abdel-Rehim et al., 2010).

The equilibrium constant for the adsorption process is related to the standard free energy of adsorption by the expression (Rawat and Singh, 1987).

$$\Delta G_{ads} = -2.303RT\log(55.5K_{ads}) \quad (7)$$

where, ΔG_{ads} is the Gibbs free energy of adsorption, T is the temperature in Kelvin and K_{ads} is the equilibrium constant for the adsorption process and 55.5 is the molar concentration of water in solution. It has been observed that the value of ΔG_{ads} for the adsorption of PVPMA on mild steel surfaces is negative (Table 3) and this value is consistent with the spontaneity of the adsorption process and the stability of the adsorbed layer on the mild steel surface (Bentiss et al., 2007). Generally, values of ΔG_{ads} up to -20 kJ mol^{-1} are consistent with the electrostatic interactions between the charged molecules and the charged metal (physisorption) while those around -40 kJ mol^{-1} or higher are associated with chemisorption as a result of sharing or transfer of electrons from polymer molecules to the metal surface to form a coordinate type of bond (Hosseini et al., 2003).The values of ΔG_{ads} indicate physical adsorption of PVPMA on mild steel surfaces. Further this assumption is supported by data obtained from the temperature dependence of the inhibition process. Inspection of Table 3 reveals that ΔG_{ads} value decreased from 28 to 22 kJ mol^{-1} with increasing temperature from 313 to 343 K.

3.2. Potentiodynamic polarization studies

Fig. 6 shows polarization curves for mild steel in 1 M HCl with and without different concentrations of PVPMA. The electrochemical parameters such as corrosion current density (I_{corr}), corrosion potential (E_{corr}), anodic and cathodic Tafel slopes (b_a and b_c) and inhibition efficiency are obtained from polarization measurements. It is evident from Table 4 that I_{corr} value decreases from 59.81×10^{-4} to 7.57 x 10^{-4} mA/cm^2 in the presence of PVPMA resulting in the efficiency of 87.34%.

A change in E_{corr} value has also been noticed in the presence of composites. According to Ferreira et al. (2004) (i) if the displacement in E_{corr} value is >85 mV, the inhibitor acts as cathodic or anodic type. (ii) if displacement in E_{corr} value is <85 mV, the inhibitor can be seen as mixed type. In the present study, maximum displacement in E_{corr} value is 36 mV, which indicates that the studied composite belongs to mixed type inhibitors. The inhibitor has first been adsorbed onto the metal surface and impeded by merely blocking the metal surface without affecting the anodic and cathodic reaction mechanisms (Abdel-Rehim et al., 2001).

As is shown in Fig. 6, the cathodic current–potential curves give rise to parallel Tafel lines, which indicate that hydrogen evolution reaction is activation controlled and that the addition of the PVPMA does not modify the mechanism of this process (Bentiss et al., 2006).The results demonstrate that the hydrogen reduction is inhibited and that the inhibition efficiency increases with inhibitor concentration. In the anodic range, the polarization curves of mild steel show that the addition of PVPMA decreases current densities in a large domain of potential. This result suggests that this compound acts as

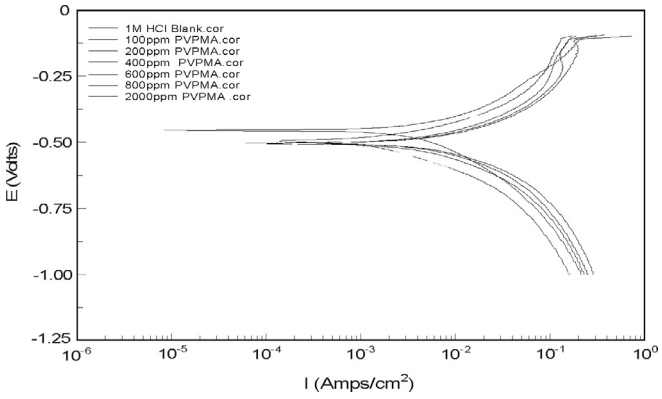

Figure 6 Polarization curves for mild steel in 1 M HCl containing different concentrations of PVPMA.

Table 4 Potentiodynamic polarization parameters for the corrosion of mild steel in 1 M HCl containing different concentrations of PVPMA.

Conc. (ppm)	E_{corr} (mv/SCE)	$I_{corr} \times 10^{-4}$ ma/cm^2	b_a (mv/dec)	b_c (mv/dec)	IE (%)	R_P (Ω cm^2)	IE (%)
Blank	−481.11	59.81	153.48	124.9		4.85	
100	−477.88	44.89	139.86	121.95	24.95	6.31	23.14
200	−478.78	43.7	154.76	127.84	26.94	6.89	29.61
400	−479.46	37.69	154.1	125.32	36.98	8.15	40.49
600	−481.42	37.08	161.7	135.36	38.00	8.81	44.95
800	−462.17	9.55	114.23	85.33	84.03	16.6	70.78
2000	−445.8	7.57	135.85	85.42	87.34	28.2	82.80

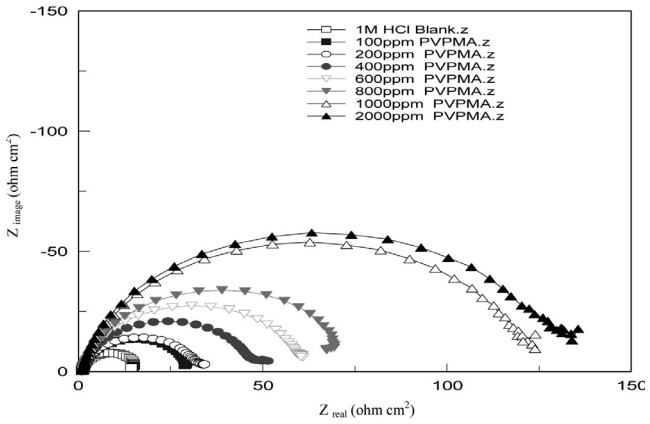

Figure 7 Nyquist diagrams for mild steel in 1 M HCl containing different concentrations of PVPMA.

Table 5 Parameters derived from the Nyquist plot of mild steel in HCl containing PVPMA.

Conc. (ppm)	R_{ct} (Ω cm^2)	IE (%)	C_{dl} (μF/cm^2)	θ
Blank	14.59		39.04	
100	29.06	49.79	22.03	0.44
200	31.74	54.03	20.17	0.48
400	46.35	68.52	13.81	0.65
600	59.5	75.48	10.76	0.72
800	71.13	79.49	9.00	0.77
1000	121.76	88.02	5.26	0.87
2000	129.96	88.77	4.93	0.87

a mixed-type inhibitor of the corrosion of mild steel in hydrochloric acid medium.

The polarization resistance measurements were performed by applying a controlled potential scan over a small range, 2 mV with respect to E_{corr}. The resulting current was linearly plotted versus potential, the slope of this plot at E_{corr} being the polarization resistance, R_p. Enhanced R_P values are observed in the presence of inhibitors. Inhibition efficiency increases with inhibitor concentration reaching a maximum (82.80%) for the highest concentration (2000 ppm) of PVPMA.

However, inhibition efficiency values that were determined using the potentio dynamic data are lower than those obtained by the weight loss method, the differences observed between these two techniques are mainly due to the different exposure times in the acid solution.

3.3. Electrochemical impedance spectroscopy

The corrosion of mild steel in acidic solution in the presence of PVPMA has been investigated by the EIS method. Nyquist diagrams for mild steel in the presence and the absence of inhibitors are shown in Fig. 7. It is apparent from these plots that the impedance response of mild steel in uninhibited HCl solution has significantly changed after the addition of PVPMA in the corrosive solution. This indicates that the impedance of inhibited substrate increases with increasing inhibitor concentration and consequently the inhibition efficiency increases.

The values of charge transfer resistance (R_{ct}) and double layer capacitance (C_{dl}) are obtained from impedance measurements. The impedance parameters and values of inhibition efficiency are given in Table 5.

The inhibition efficiency is calculated from charge transfer resistance as follows:

$$\mathrm{IE}(\%) = \frac{R_{ct(I)} - R_{ct}}{R_{ct(I)}} \times 100 \quad (8)$$

where R_{ct} and R_{ct}(I) are the charge transfer resistance values with and without inhibitor, respectively for mild steel in 1 M HCl.

It is found from Fig. 7 as PVPMA concentration increases, the R_{ct} values increase, but the C_{dl} values tend to decrease. The magnitude of R_{ct} increases while the value of C_{dl} decreases, with the addition of inhibitor which causes an increase in inhibition efficiency. The high R_{ct} values are generally associated with slower corroding systems (Samardzi ja et al., 2005). The decrease in C_{dl} value may be due to the gradual replacement of water molecules in the double layer by the adsorbed inhibitor molecules which form an adherent film on the metal surface and lead to a decrease in the local dielectric constant at the metal/solution interface.

3.4. Scanning electron microscope

The micrograph of a mild steel specimen without polymer composite shows a large number of pits and cracks due to the attack of aggressive corrosive medium (Fig. 8a). SEM micrographs of the mild steel specimen in the presence of polymer composites show a uniform layer formation on the metal surface (Fig. 8b). This suggests that PVP incorporated polymethylaniline has more surface adhesion and close packing nature (Athawale and Bhagwat, 2003). As shown in the SEM image, each

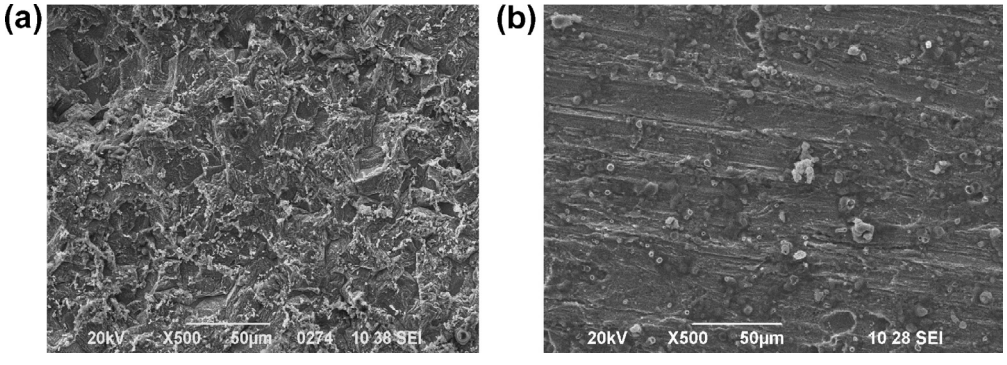

Figure 8 Scanning electron micrograph of (a) Mild steel immersed in 1 M HCl and (b) PVPMA deposited on mild steel surfaces.

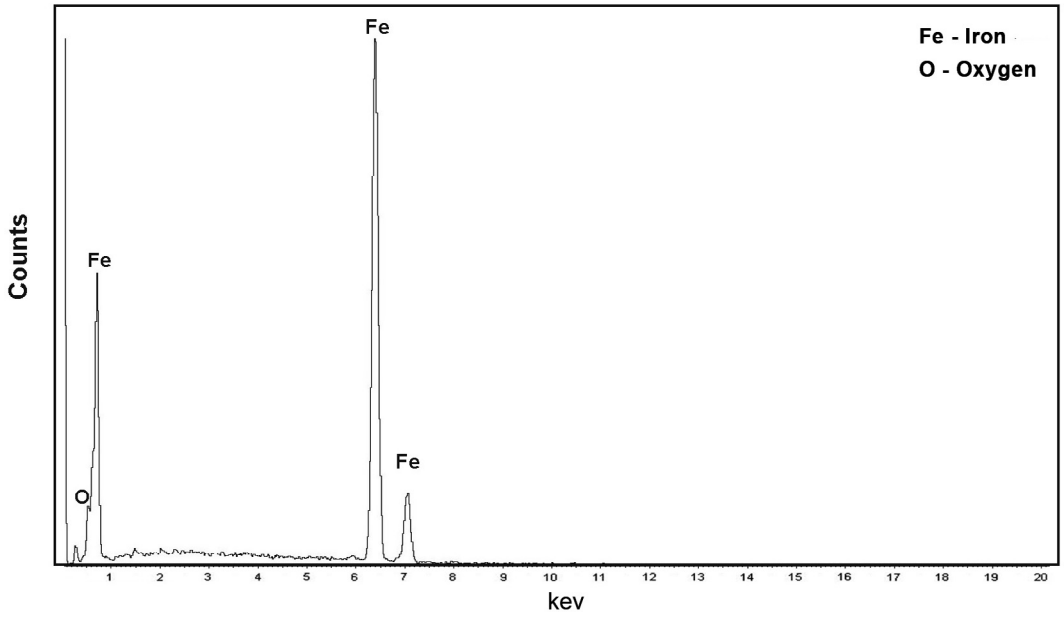

Figure 9a EDX spectra of mild steel in 1 M HCl.

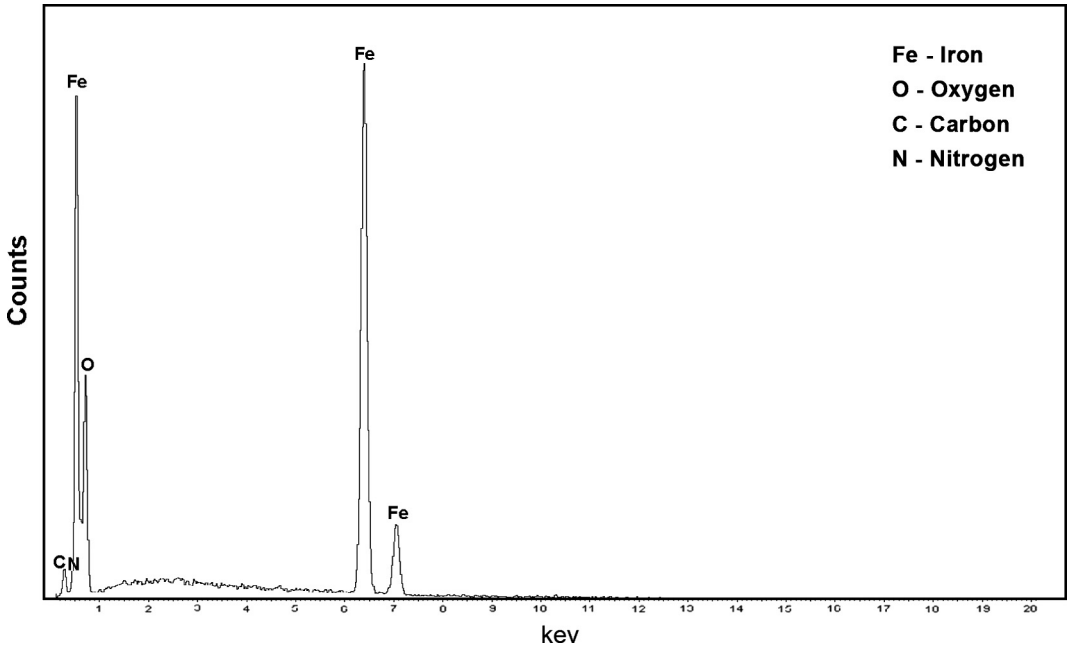

Figure 9b EDX spectra of PVPMA film deposited on mild steel surfaces.

Table 6 Percentage of atomic contents of elements in composite deposited on mild steel surfaces.

Inhibitor	Fe (%)	C (%)	O (%)	N (%)
Blank	84.15		15.85	
PVPMA	36.02	13.06	47.38	3.54

unit has many polymer granules. This might be due to the multiple nucleation of the polymer preferentially on the same site of the substrate. In some of the micrographs, it is possible to see a compact granular structure with few pores between the grains. This observation is similar to the report of polyaniline metal bilayer coating (Anandakumar et al., 2008). Further, the micrographs from SEM reveal that the surface is strongly damaged owing to corrosion in the absence of the inhibitor, but in the presence of the inhibitor there is much less damage on the surface. This is attributed to the formation of a good protective film on the mild steel surface (Migaheda et al., 2011).

3.5. Energy dispersive X-ray analysis

The protective film formed on a polished metal surface was analyzed using an EDX analysis. The strength of the iron peak in the absence and the presence of the inhibitor provides an idea about the protective film formation. The metal surface

after the exposure to polymer composites (Fig. 9b) shows the presence of nitrogen and carbon which are not present in the metal surface exposed to acid (Fig. 9a). This confirms the adsorption of polymer composite on the metal surface. By the addition of an inhibitor, the surface of mild steel is greatly protected due to the formation of an adherent film of the adsorbed polymer as indicated by a decrease of the iron peak in Fig. 8b showed that the protective film formed was strongly adherent to the surface, leading to a high degree of inhibition efficiency (Amin, 2006). The percentage of atomic contents of elements on mild steel from the EDX analysis is tabulated in Table 6.

4. Mechanism of inhibition

Corrosion inhibition of mild steel in hydrochloric acid solution by PVPMA composite can be explained on the basis of molecular adsorption. The composite inhibits corrosion by controlling both the anodic and cathodic reactions. In acidic solution the polymethyl aniline exists as protonated species. These protonated species adsorb on the cathodic sites of mild steel and decrease the evolution of hydrogen. The chloride adsorbed on the metal enhances the adsorption of the positively charged anilinium ion. The adsorption is influenced by two important factors: (1) The non polar material surrounding the positively charged nitrogen ion reduces the loss of energy due to mutual repulsion between the ions allowing a closely packed layer to form more easily and (2) the closely packed layer is further stabilized by Van der walls forces of cohesion between the alkyl chains (Sathyanarayanan et al., 1992). The adsorption on anodic sites occurs through long π electrons of aromatic rings (benzenoid and quinonoid) and a lone pair of electrons of nitrogen atoms which decreases the anodic dissolution of mild steel (Shukla et al., 2008). The high performance of the polymer is attributed to the presence of long π electron conjugation, nitrogen, oxygen atoms and larger molecular size.

5. Conclusion

The inhibition efficiencies obtained by polarization, EIS and weight loss measurements show good agreement. PVPMA is found to affect both the anodic and cathodic processes and acts as a mixed-type inhibitor. The adsorption of the inhibitor obeys the Langmuir's Isotherm and is more strictly followed by El-Awady adsorption isotherm .The negative value of ΔG_{ads} obtained from this study indicates that the studied inhibitor is strongly adsorbed on the mild steel surface and the decreasing value of ΔG with increasing temperature suggested that the adsorption of inhibitor is not favored at higher temperatures.

References

Abdel-Rehim, S.S., Sayyahb, S.M., El-Deebb, M.M., Kamalb, S.M., Azoozb, R.E., 2010. Mater. Chem. Phys. 123, 20–27.

Abdel-Rehim, S.S., Ibrahim, M.A.M., Khaled, K.F., 2001. Mater. Chem. Phys. 70, 268–273.

Afidah, A.R., Kassim, J., 2008. Recent Patents Mater. Sci. 1, 223.

Ahamad, I., Quraishi, M.A., 2009. Corros. Sci. 51, 2006–2013.

Amin, M.A., 2006. J. Appl. Electrochem. 36, 215.

Anandakumar, S., Shreemeenakshi, K., Sankaranarayanan, T.S.N., Srikanth, S., 2008. Prog. Org. Coat. 62, 285–292.

Athawale, A.A., Bhagwat, S.V., 2003. J. Appl. Polym. Sci. 89, 2412.

Bentiss, F., Bouanis, M., Mernari, B., Traisnel, M., Vezin, H., Lagrene, M., 2007. Appl. Surf. Sci. 253, 3696.

Bentiss, F., Gassama, F., Barbry, D., Gengembre, L., Vezin, H., Lagrenee, M., Traisnel, M., 2006. Appl. Surf. Sci. 252, 2684–2691.

Bentiss, F., Lebrini, M., Vezin, H., Chai, F., Traisnel, M., Lagrene, M., 2009. Corros. Sci. 51, 2165–2173.

Borole, D.D., Kapadi, U.R., Mahulikar, P.P., Hundiwale, D.G., 2006. Mater. Lett. 60, 2447–2452.

Coates, J., 2000. In: Meyers, R.A. (Ed.), Encyclopedia of Analytical Chemistry, pp. 10815–10837.

Chaturvedi, R.H., Chaudhary, R.S., 1990. Corros. Prev. Control, 53–55.

Ebenso, E.E., Alemu, H., Umoren, S.A., Obot, I.B., 2008. Int. J. Electrochem. Sci. 4, 1325.

El-Naggar, M.M., 2007. Corros. Sci. 49, 2236.

El-Taib Heakala, F., Foudab, A.S., Radwan, M.S., 2011. Mater. Chem. Phys. 125, 26–36.

Ferreira, E.S., Giancomelli, C., Giacomelli, F.C., Spinelli, A., 2004. Mater. Chem. Phys. 83, 129–134.

Gangopadhyay, R., Amitabha De Ghosh, G., 2001. Synth. Met. 123, 21–31.

Ghosh, M., Barman, A., De, S.K., Chatterjee, S., 1998. J. Appl. Phys. 84, 806–811.

Guan, N.M., Xueming, L., Fei, L., 2004. Mater. Chem. Phys. 86, 59.

Hosseini, M., Mertens, S.F.L., Arshadi, M.R., 2003. Corros. Sci. 45, 1473–1489.

Ibot, I.B., Obi-Egbedi, N.O., Umoren, S.A., 2009. Int. J. Electrochem. Sci. 4, 863.

Kokalj, A., 2010. Electrochim. Acta 56, 745.

Lagrenee, M., Mernari, B., Bouanis, M., Traisnel, M., Bentiss, F., 2002. Corros. Sci. 44, 573–588.

Lebrini, M., Bentiss, F., Vezin, H., Lagrenee, M., 2006. Corros. Sci. 48, 1291.

Migaheda, M.A., Faraga, A.A., Elsaeda, S.M., Kamala, R., Mostfab, M., Abd El-Bary, H., 2011. Mater. Chem. Phys. 125, 125–135.

Molyneux, P., 1983. Water Soluble Synthetic Polymers: Properties and Behaviour. CRC Press, New York, pp. 1, 166.

Morad, M.S., Kamal El-Dean, A.M., 2006. Corros. Sci. 48, 3398.

Nalini, D., Rajalakshmi, R., Subhashini, S., 2011. E-J. Chem. 8, 671–679.

Neoh, K.G., Kang, E.T., Tan, K.L., 1991. J. Phys. Chem. 95, 10151.

Obi-Egbedi, N.O., Obot, I.B., 2012. Arabian J. Chem. 5, 121–133.

Obot, I.B., Obi-Egbedi, N.O., Odozi, N.W., 2010. Corros. Sci. 52, 923.

Obot, I.B., Obi-Egbedi, N.O., 2010. Corros. Sci. 52, 282.

Oguzie, E.E., Njoku, V.O., Enenebeaku, C.K., Akalezi, C.O., Obi, C., 2008. Corros. Sci. 50, 3480.

Oguzie, E.E., Okolue, B.N., Ebenso, E.E., Onuoha, G.N., Onuchukwu, A.I., 2004. Mater. Chem. Phys. 87, 394.

Pritee, A.P., Gaikwad, A.B., Patil, P.P., 2007. Electrochim. Acta 52, 5958–5967.

Quraishi, M.A., Khan, S., 2005. Indian J. Chem. Technol. 12, 576–581.

Rajendran, S., Sridevi, S.P., Anthony, N., John Amalraj, A., Sundearavadivelu, M., 2005. Anti-Corros. Methods Mater. 52, 102–107.

Rawat, N.S., Singh, A.K., 1987. Bull. Electrochem. 3, 7.

Roeges, N.P.G., 1994. A Guide to the Complete Interpretation of Infrared. Spectra of Organic Structures. Wiley, New York.

Samardzi ja, K.B., Lupu, C., Hackerman, N., Barron, A.R., Luttge, A., 2005. Langmuir 21, 12187.

Sathyanarayanan, S., Dhawan, S.K., Bal Krishnan, K., 1992. Corros. Sci. 33, 1831–1841.

Shinde, V., Sainkar, S.R., Patil, P.P., 2005. Corros. Sci. 47, 1352–1369.

Shukla, S.K., Quraishi, M.A., Prakash, Rajiv., 2008. Corros. Sci 50, 2867–2872.

Singh, A., Chaudhary, R.S., 1996. Br. Corros. J. 31, 300.

Singh, A.K., Quraishi, M.A., 2009. Corros. Sci. 51, 2752–2760.

Tao, Z., Zhang, S., Li, W., Hou, B., 2009. Corros. Sci. 51, 2588.

Umoren, S.A., Ebenso, E.E., 2007. Mater. Chem. Phys. 106, 393.

Umoren, S.A., Ebenso, E.E., Okafor, P.C., Ogbobe, O., 2006. Pigm. Resin Technol. 35, 346–352.